

# Bicyclo[1.1.0]butyl Radical Cations: Synthesis and Application to [2 $\pi$ +2 $\sigma$ ] Cycloaddition Reactions

Jasper L. Tyler<sup>1,3</sup>, Felix Schäfer<sup>1,3</sup>, Huiling Shao<sup>2</sup>, Colin Stein<sup>1</sup>, Audrey Wong<sup>2</sup>, Constantin G. Daniliuc<sup>1</sup>, K. N. Houk<sup>2,\*</sup> and Frank Glorius<sup>1,\*</sup>

<sup>1</sup>Organisch-Chemisches Institut, Universität Münster, Münster, Germany.

<sup>2</sup>Department of Chemistry and Biochemistry, University of California, Los Angeles, USA.

<sup>3</sup>These authors contributed equally.

\*Correspondence to: glorius@uni-muenster.de; houk@chem.ucla.edu

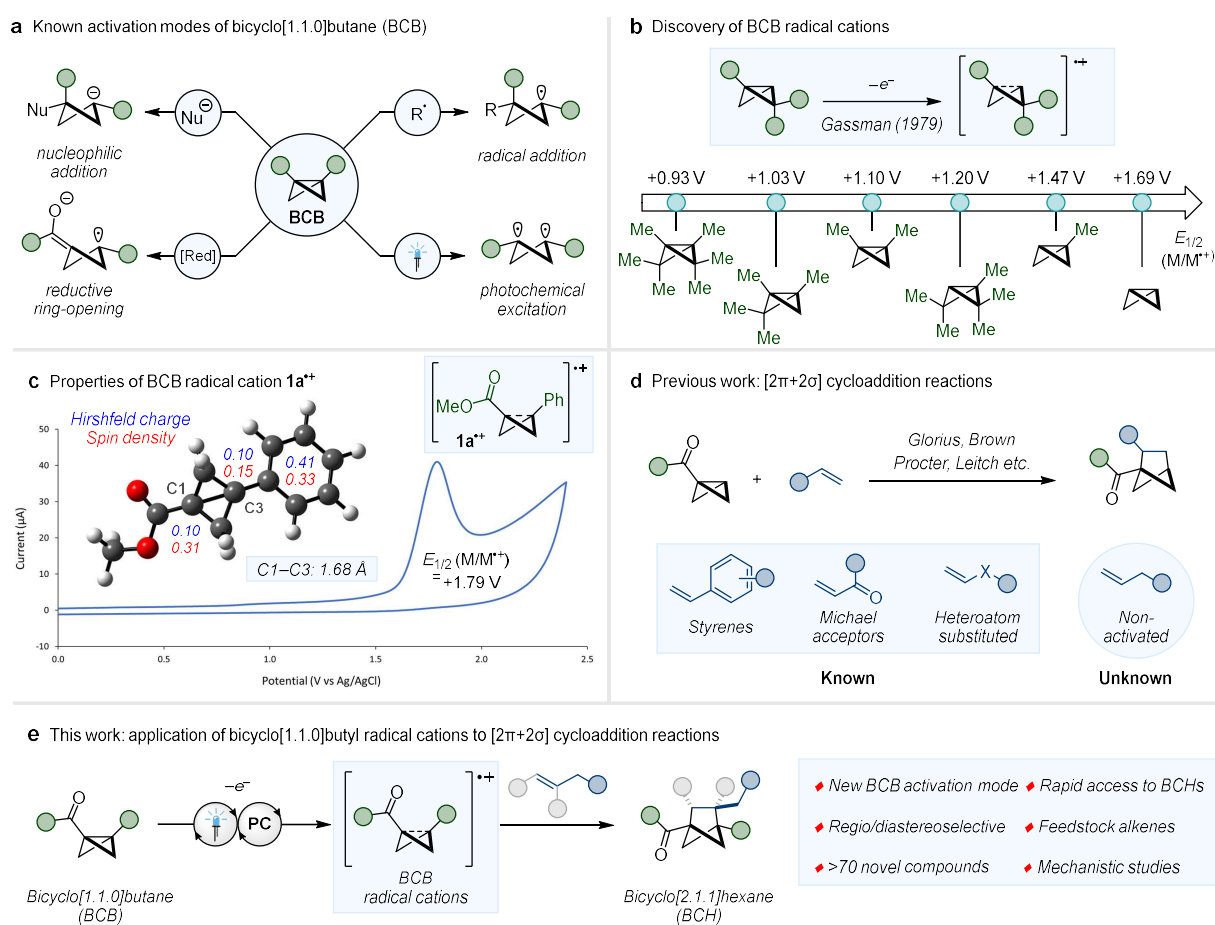
## Abstract

As the chemistry that surrounds the field of strained hydrocarbons, such as bicyclo[1.1.0]butane, continues to expand, it becomes increasingly advantageous to develop alternative reactivity modes that harness their unique properties to access new regions of chemical space. Herein, we report the use of photoredox catalysis to promote the single-electron oxidation of bicyclo[1.1.0]butanes. The synthetic utility of the resulting radical cations is highlighted by their ability to undergo highly regio- and diastereoselective [2 $\pi$ +2 $\sigma$ ] cycloaddition reactions. The most notable feature of this transformation is the breadth of alkene classes that can be employed, including non-activated alkenes, which have so far been elusive for previous strategies. A rigorous mechanistic investigation, in conjunction with DFT computation, was undertaken in order to better understand the physical nature of bicyclo[1.1.0]butyl radical cations and thus provides a platform from which further studies into the synthetic applications of these intermediates can be built upon.

## Introduction

Since its first synthesis in 1959<sup>1</sup>, bicyclo[1.1.0]butane (BCB) has captured the imagination of chemists due to its innate strain energy and relative ease of assembly and handling<sup>2,3</sup>. The highly diverse reactivity of BCB-containing compounds, facilitated by the release of strain upon breaking the bridging C1–C3 bond, has allowed such structures to become valuable building blocks for the generation of sp<sup>3</sup>-rich carbocycles and heterocycles<sup>2–5</sup>. Perhaps the most prominent reactivity mode that has been utilised in this context is the addition of nucleophiles and nucleophilic radicals to the bridgehead of electron-deficient BCB compounds (Fig. 1a).<sup>6–9</sup> In recent years, alternative strategies have also emerged, such as electrophilic addition<sup>10–12</sup>, reduction<sup>13,14</sup> or Lewis acid activation<sup>15–18</sup> of adjacent carbonyl fragments to trigger ring-

30 opening, pyridine-boryl radical transfer<sup>19,20</sup> and photochemical excitation of the strained bridging bond to  
 31 access the corresponding diradical<sup>21,22</sup>. Employing these strategies has led to the development of many  
 32 unique transformations and, as a consequence, BCB-containing compounds have become cemented as  
 33 valuable tools in areas such as bioconjugation<sup>23,24</sup> and in the assembly of challenging arene isosteres<sup>10,11,25</sup>.  
 34 However, in order to find new applications and access unexplored regions of chemical space, alternative  
 35 reactivity modes that harness the unique properties of BCBs are required.



36

37 **Fig. 1 | Bicyclo[1.1.0]butyl radical cations for the synthesis of bicyclo[2.1.1]hexanes.** **a** Known activation modes of  
 38 bicyclo[1.1.0]butane. **b** Discovery of the direct oxidation of substituted bicyclo[1.1.0]butane compounds<sup>26</sup>. **c** Oxidation potential  
 39 of BCB **1a** vs Ag/AgCl (2 M LiCl in EtOH) and physical properties of bicyclo[1.1.0]butyl radical cation **1a<sup>++</sup>**. **d** Previous reports of  
 40  $[2\pi+2\sigma]$  cycloaddition reactions. **e** This work: application of bicyclo[1.1.0]butyl radical cations to  $[2\pi+2\sigma]$  cycloaddition reactions.

41 In 1979, Gassman reported a study on the relationship between alkyl substitution and the ease of  
 42 oxidation of strained hydrocarbons<sup>27</sup>. By measuring the half-wave potentials of a variety of substituted  
 43 bicyclo[1.1.0]butanes, it was demonstrated that the  $\sigma$ -framework of the bicycle could readily undergo  
 44 single-electron oxidation to the corresponding radical cation (Fig. 1b)<sup>26</sup>. Despite this discovery, the  
 45 synthetic potential of bicyclo[1.1.0]butyl radical cations has been severely underexplored<sup>28</sup>, with non-

46 selective nucleophilic ring-opening being the only transformation demonstrated for these  
47 intermediates<sup>29–31</sup>. We therefore determined to assess the feasibility of single-electron oxidation as a  
48 strategy to access new bicyclo[1.1.0]butane reactivity.

49 To avoid the issues associated with handling low-molecular-weight strained hydrocarbons, electron-  
50 deficient BCB **1a**, known to be non-volatile and easily synthesised, was investigated (Fig. 1c). Although this  
51 species contains an electron-withdrawing group directly appended to the  $\sigma$ -framework, cyclic  
52 voltammetry studies clearly showed that this compound could be oxidised, with a half-wave potential of  
53 +1.79 V vs Ag/AgCl (2 M LiCl in EtOH). Density functional theory (DFT) calculations of the condensed  
54 Hirshfeld charges and spin densities of the radical cation revealed that both the overall charge and the  
55 spin were largely delocalised across the bridging bond of the BCB framework as well as the aromatic ring  
56 (Fig. 1c). Analysing these values revealed that the C1 and C3 carbon atoms have a greater contribution of  
57 the overall spin (0.31 and 0.15, respectively) compared to the positive charge (0.10 and 0.10, respectively),  
58 which is more concentrated on the aryl ring (0.41). Additionally, the bridging bond remains intact upon  
59 oxidation and shows an elongation of just 0.16 Å compared to the ground state<sup>32</sup>, highlighting the  
60 difference between this activation strategy and energy transfer, where  $\sigma$ -bond cleavage to form the  
61 corresponding diradical occurs<sup>21</sup>.

62 With an understanding of the accessibility and physical properties of BCB radical cations, a reactivity  
63 regime that cannot be achieved using previously known strategies was pursued. Specifically, we targeted  
64  $[2\pi+2\sigma]$  cycloaddition reactions to access bicyclo[2.1.1]hexane (BCH) compounds, highly valuable  
65 isosteres of *ortho*- and *meta*-substituted benzene that are  $sp^3$ -rich with well-defined substituent exit  
66 vectors<sup>33–36</sup>. Although  $[2\pi+2\sigma]$  cycloaddition reactions that harness the strained bond of BCB have been  
67 reported by our own research group<sup>18,37–39</sup>, as well as those of Brown<sup>21</sup>, Procter<sup>13</sup>, Leitch<sup>25</sup> and others<sup>14–</sup>  
68 <sup>17,19,20,40</sup>, in all cases, alkenes that can be employed require either a radical stabilising group,  
69 electron-withdrawing group or heteroatom directly appended to the double bond, depending on the  
70 respective mechanism (Fig. 1d). Conversely, it is known that styrene-type radical cations<sup>41–43</sup>,  
71 intermediates that display remarkably similar levels of charge and spin delocalisation to **1a**<sup>•+</sup> (see  
72 Supplementary Information for details), have the ability to participate in  $[2\pi+2\pi]$  cycloaddition reactions  
73 with olefins that are not stabilised by an adjacent  $\pi$ -system or carbonyl unit<sup>44–46</sup>. Therefore, we believed  
74 that harnessing BCB radical cations could provide a general method for  $[2\pi+2\sigma]$  cycloaddition reactions,  
75 allowing the transformation to occur with multiple distinct classes of olefins, including simple feedstock  
76 alkenes that have so far been elusive.

77        Herein, we report the successful application of bicyclo[1.1.0]butyl radical cations to  $[2\pi+2\sigma]$   
78 cycloaddition reactions to generate a unique selection of BCH structures (Fig. 1e). The most notable  
79 features of this strategy are the breadth of alkene classes that can be employed and the remarkable levels  
80 of regio- and diastereoselectivity that can be achieved using single-electron oxidation as the activation  
81 mode for BCB. A rigorous experiment-based mechanistic study, in conjunction with DFT computation, was  
82 undertaken in order to better understand this process and illuminate how these strained radical cations  
83 interact with alkenes. Consequently, we believe that the work described here can serve as a platform from  
84 which further studies into the potential synthetic applications of BCB radical cations can be built upon.

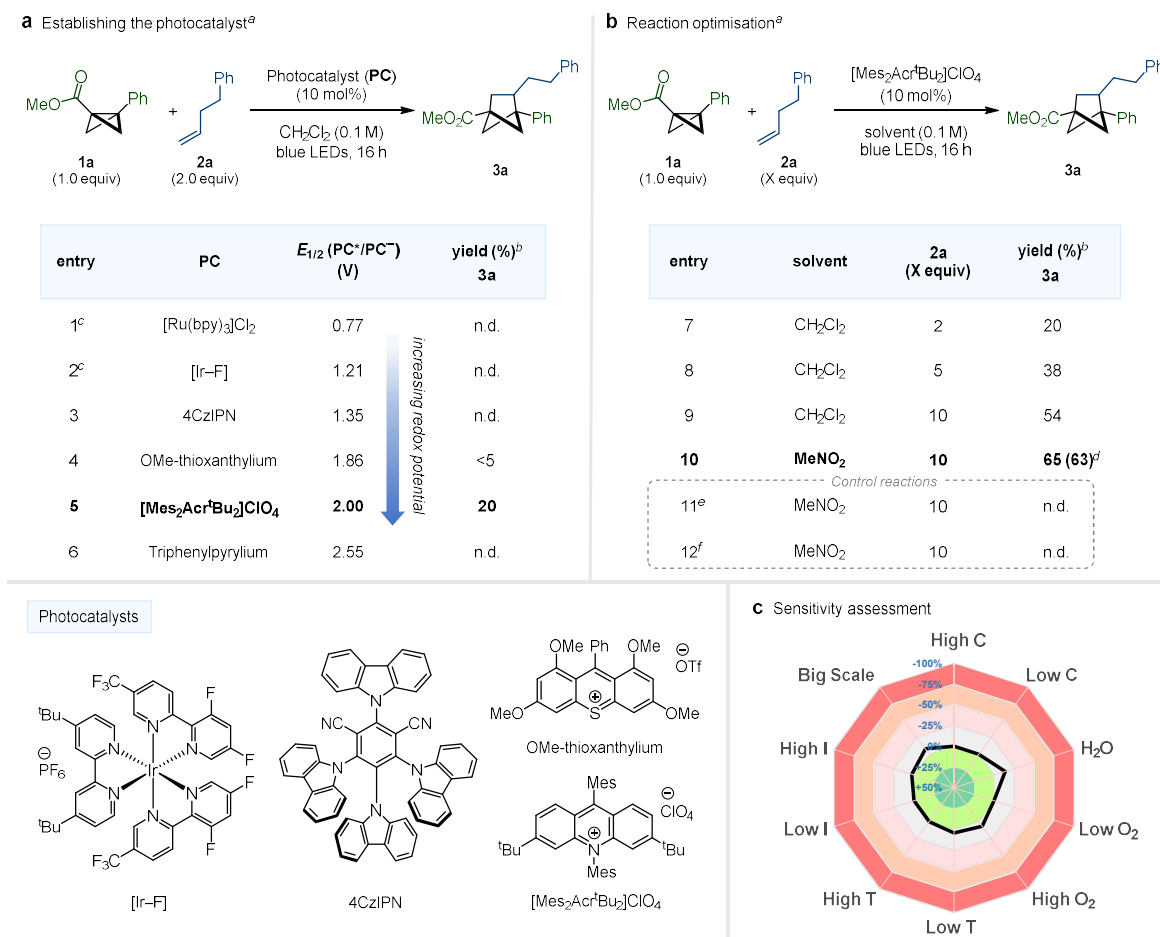
## 85 **Results and Discussion**

### 86 **Reaction development**

87        Our investigation commenced with the exploration of suitable photocatalysts, capable of promoting  
88 the single-electron oxidation of the BCB moiety. Olefin **2a**, containing no adjacent heteroatom or radical  
89 stabilising group, was selected as the model coupling partner due to its presumed inactivity under any  
90 currently known BCB  $[2\pi+2\sigma]$  cycloaddition conditions. Upon screening photocatalysts across a wide  
91 range of oxidation potentials, it was demonstrated that  $[\text{Mes}_2\text{Acr}^t\text{Bu}_2]\text{ClO}_4$  ( $E_{1/2}(\text{PC}^*/\text{PC}^\bullet) = +2.00$  V vs  
92 SCE)<sup>47</sup>, irradiated with blue LEDs, could catalyse the desired  $[2\pi+2\sigma]$  cycloaddition reaction with **2a**  
93 (Fig. 2a, entry 5). Indeed, it was observed that employing photocatalysts that display an excited state  
94 oxidation potential below +1.86 V (or significantly greater than +2.00 V) failed to deliver any observable  
95 product (entries 1-6). After an extensive exploration of the reaction conditions (see Supplementary  
96 Information for full optimisation details), it was found that improvements to the yield could be achieved  
97 upon increasing the equivalents of the alkene coupling partner and performing the reaction in  $\text{MeNO}_2$   
98 (Fig. 2b, entries 7-10). Although this reaction represents the first example of a bicyclo[1.1.0]butane  
99  $[2\pi+2\sigma]$  cycloaddition with a simple alkyl substituted alkene, the overall yield is partially limited by the  
100 side reactions that can occur from the BCB radical cation, such as dimerisation<sup>30,31</sup>. Finally, control  
101 reactions, in which the photocatalyst and light source were omitted, were performed (entries 11-12). The  
102 inability to access any cycloaddition product under these conditions clearly shows that product formation  
103 is dependent on the generation of the excited state photocatalyst and does not arise as a result of direct  
104 excitation of either the BCB or alkene substrates.

105        In order to assess the robustness and reproducibility of the newly established protocol, a reaction  
106 condition-based sensitivity assessment was performed (Fig. 2c)<sup>48</sup>. Interestingly, the reaction was shown  
107 to be remarkably tolerable towards perturbations in the temperature (T), concentration (c), oxygen level

108 and light intensity (I), with only a slight decrease in yield observed when H<sub>2</sub>O was added to the reaction  
 109 mixture. Additionally, the photocatalysed reaction could be performed on 4.0 mmol scale, showing a  
 110 relatively small erosion in isolated yield compared to the standard reaction (53% vs 63%).



111 **Fig. 2 | Optimisation of the BCB radical cation [2π+2σ] cycloaddition reaction.** **a** Establishing the photocatalyst.  
 112 [Mes<sub>2</sub>Ac<sup>r</sup>Bu<sub>2</sub>]<sup>+</sup>ClO<sub>4</sub><sup>-</sup> was observed to effectively promote the desired [2π+2σ] cycloaddition reaction. **b** Optimisation of the reaction  
 113 conditions. MeNO<sub>2</sub> and a 10:1 ratio of alkene to BCB were determined to be the optimal conditions. **c** Sensitivity assessment of  
 114 the reaction conditions, demonstrating that the presence of water has the largest impact on reaction outcome. <sup>a</sup>Reactions  
 115 performed on 0.05 mmol scale under blue LED (λ<sub>max</sub> = 425 nm) irradiation. <sup>b</sup>Yields determined by <sup>1</sup>H NMR of the crude reaction  
 116 mixture using CH<sub>2</sub>Br<sub>2</sub> as an internal standard. <sup>c</sup>2 mol% of photocatalyst. <sup>d</sup>Isolated yield on 0.2 mmol scale. <sup>e</sup>No photocatalyst.  
 117 <sup>f</sup>Reaction performed in absence of light.

118

## 119 Reaction scope

120 With the optimised reaction conditions in hand, the scope of the reaction with respect to the olefin was  
 121 systematically investigated to both assess the generality of the transformation and to discover the limits  
 122 of reactivity (Table 1). As well as the simple hydrocarbon 1-hexene (**3b**), propene gas could also be  
 123 employed under the same reaction conditions to access **3c** in 38% yield. Additionally, functional groups

124 such as primary halides (**3d-e**), terminal alkynes (**3f**), ketones (**3g**), ethers (**3h**), esters (**3i**), internal alkynes  
125 (**3j**), thiophenes (**3k**) sulfones (**3l**), quinolines (**3m**), phthalimides (**3n**) and amino acid derivatives (**3o**) were  
126 all compatible with the transformation and provided a single regioisomer of the desired products.  
127 However, limitations to the reaction were discovered when it was observed that some nucleophilic  
128 fragments such as unprotected alcohols and amines could not be tolerated in the alkene fragment (see  
129 Supplementary Information for all failed substrates).

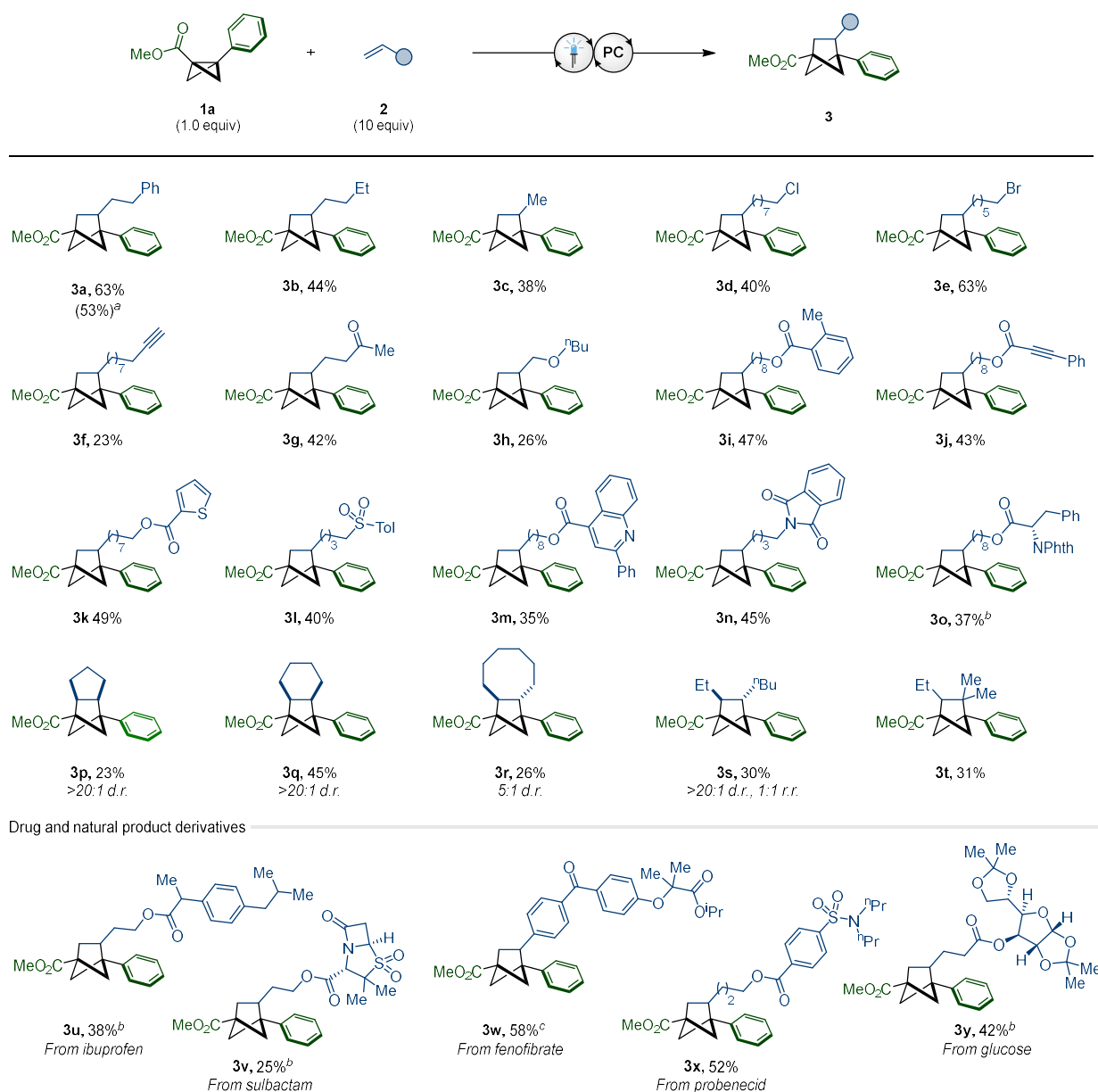
130 Exploring the scope of the alkene substitution pattern demonstrated that internal alkenes such  
131 as cyclopentene and cyclohexene could be used to access BCH structures **3p** and **3q** exclusively as the  
132 *cis*-diastereomer. However, increasing the ring size to cyclooctene resulted in isomerisation to the *trans*-  
133 isomer (**3r**). Pleasingly, non-cyclic 1,2-disubstituted alkenes such as (*E*)-oct-3-ene were also compatible,  
134 providing **3s** in 30% yield as a single diastereomer. Unsurprisingly, with no significant electronic or steric  
135 bias, a mix of regioisomers was observed for this substrate. On the other hand, when trisubstituted alkene  
136 2-methylpent-2-ene was utilised, only a single regioisomer (**3t**) was detected in the reaction mixture,  
137 demonstrating the ability of the system to clearly distinguish between mono- and disubstituted sp<sup>2</sup> carbon  
138 atoms.

139 Given that bicyclo[2.1.1]hexane structures are seen as potential sp<sup>3</sup>-rich isosteres for *ortho*- and  
140 *meta*-substituted benzene, we next investigated the tolerance of natural product and approved  
141 pharmaceutical derived alkenes in the newly developed [2π+2σ] cycloaddition reaction. Promisingly,  
142 substrates derived from the anti-inflammatory drug ibuprofen (**3u**) and the β-lactamase inhibitor  
143 sulbactam (**3v**) could be tolerated. In addition, derivatives of the cholesterol lowering pharmaceutical  
144 fenofibrate (**3w**), the gout medication probenecid (**3x**) and a protected glucose analogue (**3y**) were all  
145 capable of accessing the desired BCH products. As complex alkene substrates could be deemed more  
146 precious than the BCB coupling partner, we also demonstrated that inverting the stoichiometry of this  
147 reaction to have the olefin as the limiting reagent, could also provide access to the desired products in  
148 comparable yields (see Supplementary Information for details).

149 Initially, we hypothesised that the extension of the transformation to include “activated” alkenes,  
150 such as styrenes, would be challenging, as these compounds are known to be susceptible to oxidation by  
151 the photocatalyst. Although this was indeed observed, styrene-type substrates typically exhibited an  
152 improved yield in the reaction due to their enhanced reactivity with the BCB radical cation (Table 2).

153

154 **Table 1 | Bicyclo[1.1.0]butane [ $2\pi+2\sigma$ ] cycloaddition reaction with non-activated alkenes**



155

156 Reaction conditions: **1a** (0.2 mmol), **2** (2.0 mmol), [Mes<sub>2</sub>Acr<sup>t</sup>Bu]<sub>2</sub>ClO<sub>4</sub> (10 mol%), MeNO<sub>2</sub> (0.1 M), blue LEDs ( $\lambda_{\text{max}} = 425 \text{ nm}$ ), 16 h.  
 157 Isolated yields given. The *d.r.* and *r.r.* values were determined by <sup>1</sup>H NMR analysis of the crude reaction mixture. <sup>a</sup>Reaction  
 158 performed on 4.0 mmol of **1a**. <sup>b</sup>Substrates that contain a pre-existing stereocentre were formed as a 1:1 mix of diastereomers.  
 159 <sup>c</sup>Using conditions from Table 2 (see below).

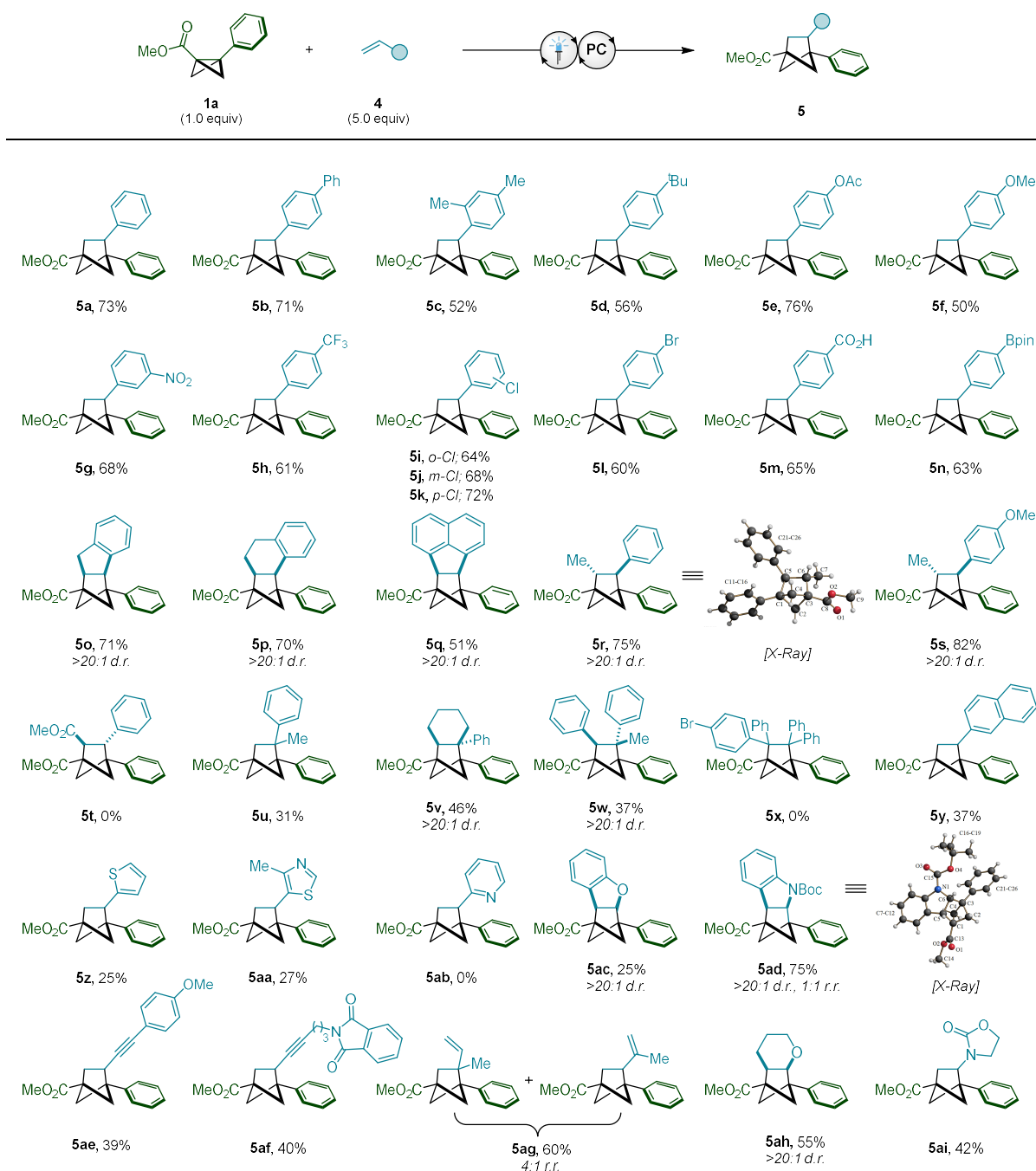
160 Despite involving a direct interaction with an electron-deficient radical cation intermediate, styrene-type  
 161 alkenes bearing both electron-donating and electron-withdrawing groups were viable in this  
 162 transformation, and all delivered the desired products as single regioisomers (**5a-h**). Additionally, highly  
 163 versatile functional handles such as halides (**5i-l**), carboxylic acids (**5m**) and boronic esters (**5n**) could also

164 be tolerated under the reaction conditions, providing the potential for further derivatisation of these  
165 substrates. When exploring the effect of alkene substitution, it was again observed that cyclic  
166 1,2-disubstituted substrates are capable of accessing the desired BCH products, exclusively as the  
167 *cis*-diastereomer (**5o-q**). In the case of acyclic (*E*)-1,2-disubstituted olefins, only the *trans*-isomer is  
168 detected (**5r-s**), with the stereochemistry confirmed by X-ray crystallography. The limit of reactivity was  
169 located when highly electron-deficient Michael-type alkenes were observed to be unsuitable for this  
170 transformation (**5t**), making this approach complementary to previously reported radical-based BCB  
171 [2 $\pi$ +2 $\sigma$ ] cycloaddition reactions<sup>13,14,19</sup>. However, subjecting 1,1-disubstituted and trisubstituted alkenes  
172 to the newly developed reaction conditions could provide access to highly substituted BCH substrates **5u**,  
173 **5v** and **5w**, although tetrasubstituted alkenes were too sterically hindered to deliver the desired  
174 cycloadduct (**5x**).

175 One of the key drawbacks of previously reported BCB [2 $\pi$ +2 $\sigma$ ] cycloaddition reactions is the  
176 limited generality with respect to the alkene coupling partner and so we next turned our attention to  
177 other classes of olefin which could be employed. In addition to vinyl naphthalene (**5y**), heterocycles  
178 containing Lewis basic atoms such as vinyl thiophene (**5z**) and thiazole (**5aa**) were amenable to the  
179 cycloaddition reaction, although vinyl pyridine was deemed unsuitable (**5ab**). Interestingly, this  
180 transformation could also be used to facilitate the dearomatisation of heterocycles such as benzofuran  
181 (**5ac**) and indole (**5ad**), as well as being compatible with enynes (**5ae-af**), dienes (**5ag**), enol ethers (**5ah**)  
182 and enamine-type substrates (**5ai**). These results demonstrate the remarkable variety of olefins that can  
183 interact with BCB radical cations and highlight the inimitable reactivity of this synthetic intermediate.

184 When exploring the electronic effect of the BCB fragment, we were eager to discover whether a  
185 relationship between the aptitude for cycloaddition and the compound oxidation potential could be  
186 established (Table 3). Firstly, it was discovered that BCB substrates which do not bear an  
187 electron-withdrawing group possess a considerably lower oxidation potential and yield only trace product  
188 under the developed cycloaddition conditions (**5aj**). However, ester and amide containing BCB  
189 compounds bearing aryl substitution that did not greatly perturb the substrate oxidation potential, could  
190 effectively deliver the desired BCH products (**5ak-am**). Considerably decreasing the electron density of  
191 the aromatic system, through the addition of a trifluoromethyl group, resulted in a BCB compound with  
192 an oxidation potential of +2.00 V which failed to deliver the desired cycloadduct and thus represents the  
193 upper limit of BCB oxidation by [Mes<sub>2</sub>Acr<sup>t</sup>Bu<sub>2</sub>]<sub>2</sub>ClO<sub>4</sub> under these conditions (**5an**).

194

Table 2 | Bicyclo[1.1.0]butane [ $2\pi+2\sigma$ ] cycloaddition reaction with activated alkenes

196

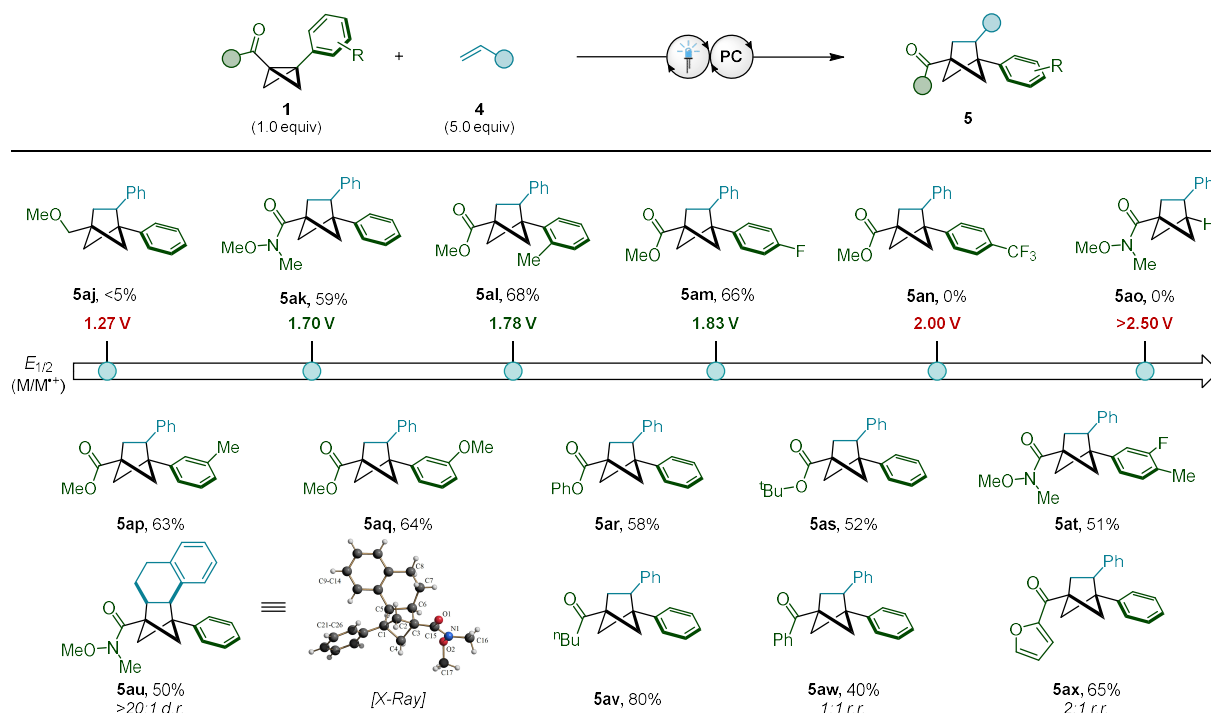
197 Reaction conditions: **1a** (0.2 mmol), **4** (1.0 mmol), [Mes<sub>2</sub>Acr<sup>t</sup>Bu<sub>2</sub>]<sub>2</sub>ClO<sub>4</sub> (10 mol%), MeCN (0.1 M), blue LEDs ( $\lambda_{\text{max}} = 425 \text{ nm}$ ), 16 h.  
 198 Isolated yields given. The *d.r.* and *r.r.* values were determined by <sup>1</sup>H NMR analysis of the crude reaction mixture.

199 It must also be stated that removal of the aryl ring entirely resulted in a drastic increase in  
 200 oxidation potential (**5ao**), presumably due to the inability of the corresponding radical cation to delocalise  
 201 into the aromatic system. From the data obtained from these cyclic voltammetry studies, a redox window

202 for reactivity was established allowing BCB compounds to first be analysed using this technique and then  
 203 only be employed if their oxidation potential falls within this potential range. Using this guiding principle,  
 204 a variety of aryl substitution patterns, different ester groups, amides and ketones were all shown to be  
 205 suitable substrates in this transformation (**5ap-ax**).

206

207 **Table 3 | Effect of BCB oxidation potential on the [2π+2σ] cycloaddition reaction**



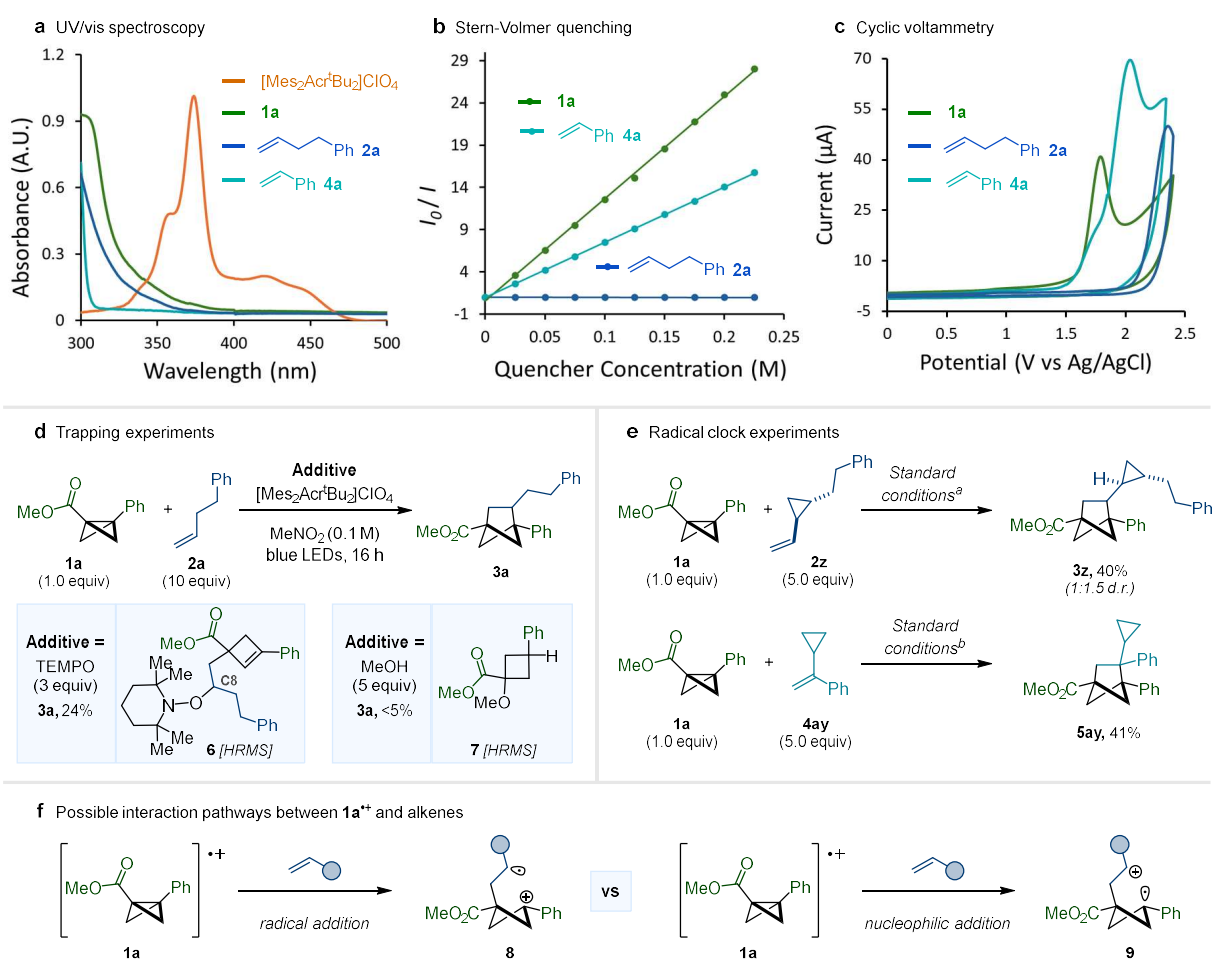
208

209 Reaction conditions: **1a** (0.2 mmol), **4** (1.0 mmol), [Mes<sub>2</sub>Acr<sup>+</sup>Bu<sub>2</sub>]<sup>-</sup>ClO<sub>4</sub> (10 mol%), MeCN (0.1 M), blue LEDs ( $\lambda_{\text{max}} = 425 \text{ nm}$ ), 16 h.  
 210 Isolated yields given. Oxidation potentials of the corresponding BCB starting materials are given in MeCN against the Ag/AgCl  
 211 electrode (2 M LiCl in EtOH). The *d.r.* and *r.r.* values were determined by <sup>1</sup>H NMR analysis of the crude reaction mixture.

## 212 Mechanistic studies

213 To confirm that BCB radical cation **1<sup>•+</sup>** is indeed responsible for reactivity, and to establish the mechanism  
 214 of the [2π+2σ] cycloaddition reaction, we set about designing experiments that could provide a deeper  
 215 understanding of the transformation described. Firstly, UV/vis spectroscopy of the individual reaction  
 216 components revealed that the photocatalyst [Mes<sub>2</sub>Acr<sup>+</sup>Bu<sub>2</sub>]<sup>-</sup>ClO<sub>4</sub> is the only light absorbing species at  
 217  $\lambda = 425 \text{ nm}$ , confirming that direct excitation of either BCB **1a** or alkene **2a** cannot be responsible for  
 218 reactivity (Fig. 3a). Furthermore, Stern–Volmer quenching studies clearly demonstrated that BCB **1a** is an  
 219 effective quencher of the photocatalyst excited state, whereas alkene **2a** gave no indication that it can  
 220 interact with this excited state species (Fig. 3b). However, quenching was detected, albeit to a lesser

221 extent than for **1a**, upon the addition of styrene (**4a**). These observations are in full corroboration with  
 222 the cyclic voltammetry (CV) experiments that were performed (Fig. 3c). Here, both BCB **1a** (+1.79 V vs  
 223 Ag/AgCl) and styrene **4a** (+2.03 V vs Ag/AgCl) show oxidation peaks that were deemed accessible for the  
 224 photocatalyst excited state, whereas **2a** was observed to have an oxidation potential well outside this  
 225 range (+2.36 V vs Ag/AgCl). Additionally, the quantum yield for the standard reaction was calculated to be  
 226  $\phi = 3.7$ , revealing that this cycloaddition reaction can proceed via a radical chain mechanism.



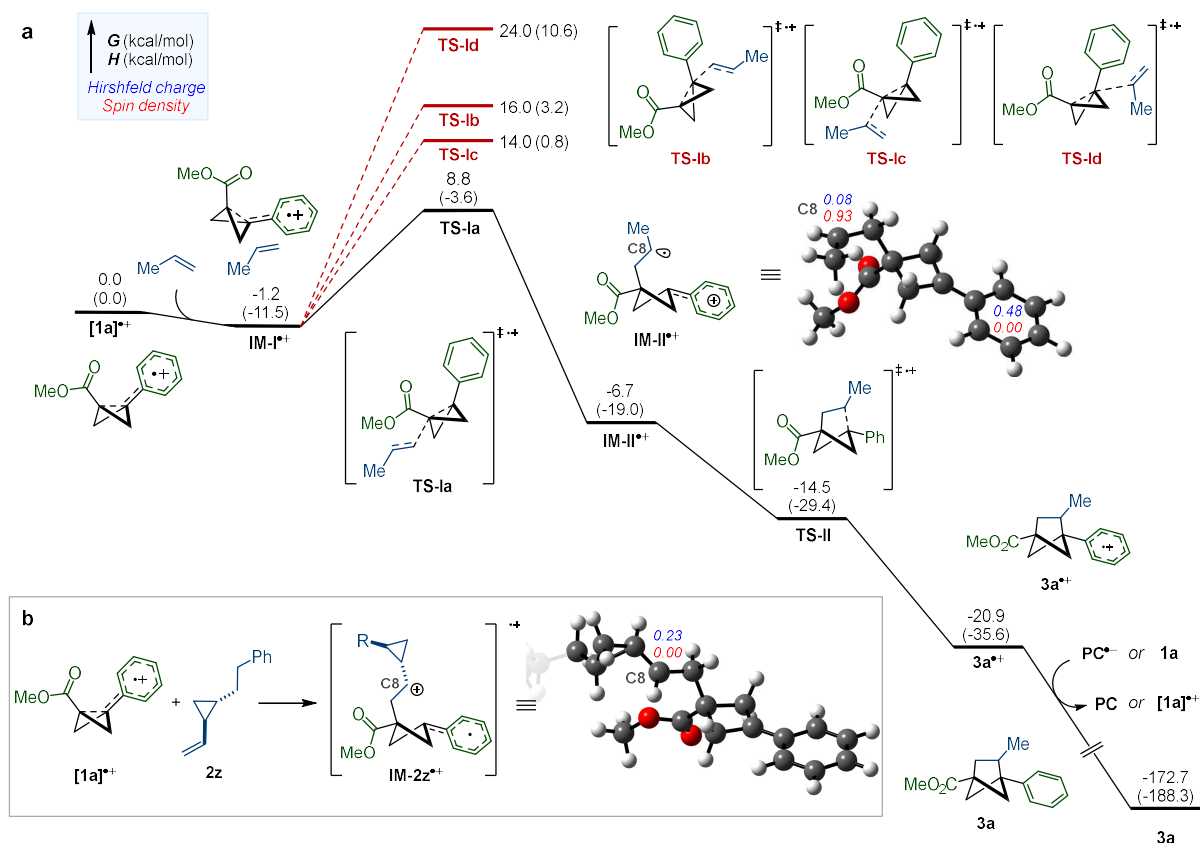
227  
 228 **Fig. 3 | Mechanistic studies.** **a** Ultraviolet–visible absorption spectra of the reaction components, showing that the photocatalyst  
 229 is the only absorbing species near the excitation wavelength ( $\lambda_{\text{max}} = 425 \text{ nm}$ ). **b** Stern–Volmer quenching studies. Analysis revealed  
 230 that the luminescence emission of the photocatalyst was quenched efficiently by BCB **1a** and also styrene **4a**, whereas no  
 231 quenching was observed with **2a**. **c** Cyclic voltammetry measurements versus the Ag/AgCl reference electrode (2 M LiCl in EtOH).  
 232 Oxidation of **1a** and **4a** was observed at +1.79 V and +2.03 V respectively which suggest that these two compounds can be oxidised  
 233 by the excited state photocatalyst ( $E_{1/2} [\text{PC}^+]/[\text{PC}]^- = +2.0 \text{ V vs SCE}$ ). **2a** was observed to oxidise at +2.36 V, indicating that the  
 234 excited state photocatalyst cannot oxidise this species under the reaction conditions. **d** Trapping experiments. 2,2,6,6-  
 235 Tetramethylpiperidinyloxy (TEMPO) was observed to partially inhibit the reaction, whereas MeOH completely suppresses product  
 236 formation. Trapping adducts **6** and **7** were observed by HRMS and the structures were assigned using NMR spectroscopy. **e** Radical  
 237 clock experiments gave no evidence of cyclopropane ring opening. <sup>a</sup>Standard conditions from Table 1. <sup>b</sup>Standard conditions from  
 238 Table 2. **f** Potential intermediates arising from the interaction of **1a\*\*** and an alkene.

239 Overall, these results strongly suggest that, in the case of non-activated alkenes, BCB radical  
240 cation **1<sup>•+</sup>** acts as the key intermediate in the [2 $\pi$ +2 $\sigma$ ] cycloaddition reaction. Despite undergoing oxidation  
241 by the photocatalyst, radical cations arising from styrene-type alkenes were found, during DFT studies, to  
242 be unable to lead to product formation and so this alternative pathway could be eliminated as a possibility  
243 (see Supplementary Information for details).

244 Given that the oxidation of the bicyclobutane framework constitutes an activation mode that has  
245 been underexplored in synthesis, trapping studies and radical clock experiments were next conducted to  
246 probe their effect on the reaction outcome. Surprisingly, when radical trapping agent TEMPO was added  
247 to the standard reaction, product formation was not entirely suppressed, whereas the addition of MeOH  
248 resulted in only trace product being observed (Fig. 3d). In the case of TEMPO, the observation of a 1:1:1  
249 trapping adduct (assigned as structure **6**), suggests that a carbon-centred radical is localised at the C8  
250 position. To confirm the presence of this intermediate, cyclopropane-containing alkenes **2z** and **4ay** were  
251 subjected to standard reaction conditions. However, no cyclopropane ring opening could be detected in  
252 either case and cycloadducts **3z** and **5ay** were isolated in 40% and 41% yield, respectively (Fig. 3e). From  
253 these apparently contradictory results it was unclear whether the initial interaction of the BCB radical  
254 cation and the alkene proceeds via radical addition to give an intermediate of type **8**, or occurs via alkene  
255 nucleophilic addition (**9**, Fig. 3f). Therefore, we turned to computational calculations to provide key  
256 insights into the operative mechanism.

### 257 **DFT Calculations**

258 When employing density functional theory (DFT) calculations to further study the reaction pathway, it  
259 was observed that the complexation of the radical cation **1a<sup>•+</sup>** with a simple alkene (propene) to form  
260 **IM-I<sup>•+</sup>**, is exergonic by 1.2 kcal/mol (Fig. 4a). Subsequent insertion of the alkene fragment into the BCB  
261 scaffold was found to be a kinetically facile process (**TS-Ia**), with a free energy barrier of 10.0 kcal/mol  
262 with respect to the preceding **IM-I<sup>•+</sup>**. To rationalise the regiochemistry of this initial bond forming process,  
263 all other possible transition states (**TS-Ib**, **TS-Ic**, and **TS-Id**) were computed and were all found to have  
264 significantly higher free energy barriers. From **TS-Ia**, formation of the subsequent intermediate **IM-II<sup>•+</sup>** was  
265 determined to be exergonic by 5.5 kcal/mol.



266

267 **Fig. 4 | Computational mechanistic investigations.** **a** Computed reaction coordinate profile of the  $[2\pi+2\sigma]$  cycloaddition reaction  
 268 between BCB radical cation  $1a^{•+}$  and propene; **b** Computed spin densities and Hirshfeld charges of radical clock intermediate  
 269  $IM-2z^{•+}$ . All DFT calculations were conducted at either  $\omega$ b97xd/def-TZVPP/CPCM (solvent = MeCN) or  $\omega$ b97xd/def2SVP/CPCM  
 270 (solvent = MeCN) levels of theory (see Supplementary Information for full details).

271 Upon closer analysis of  $IM-II^{•+}$  we identified that the spin density of the radical cation is highly  
 272 localised on the propene  $\alpha$ -carbon (C8), a result that agreed with the outcome of the radical trapping  
 273 experiments which suggested that a carbon radical is present at this position (Fig. 3d). However, in order  
 274 to rationalise the apparently contradictory results of the radical clock experiments, we calculated the spin  
 275 densities for the corresponding intermediate with substrate  $2z$  ( $IM-2z^{•+}$ , Fig. 4b) and found that, in this  
 276 case, no spin density is localised on the carbon adjacent to the cyclopropane (C8). From this, we can  
 277 conclude that the distribution of spin and charge density in the intermediate following the initial  
 278 interaction of  $1a^{•+}$  with olefins is highly dependent on the nature of the alkene substituents. The final C–C  
 279 bond formation step in the mechanism ( $TS-II$ ) was found to be a barrierless process, with an estimated  
 280 free energy of  $-14.5$  kcal/mol using a restrained calculation (see Supplementary Information). Reduction  
 281 of the thermodynamically stable  $3a^{•+}$  ( $-20.9$  kcal/mol), can then occur either the reduced  
 282 photocatalyst or a neutral BCB molecule to turn over the radical chain and generate BCH product  $3a$ .

283

## 284 Conclusion

285 In conclusion, we have identified a new strategy for the single-electron oxidative activation of  
286 bicyclo[1.1.0]butane via photoredox catalysis. The synthetic utility of the resulting radical cation was  
287 highlighted by its ability to undergo  $[2\pi+2\sigma]$  cycloaddition reactions in a highly regio- and  
288 diastereoselective fashion. The scope of the transformation with respect to the alkene coupling partner  
289 was remarkably broad, allowing the cycloaddition of styrene-type, heteroatom substituted and, for the  
290 first time in this reaction class, non-activated alkenes. A comprehensive experimental and computational  
291 mechanistic study was undertaken that confirmed the involvement of BCB radical cations and illuminated  
292 the nature of their interaction with olefins. We foresee that the work presented above can serve as a  
293 platform from which further studies into the potential synthetic applications of bicyclo[1.1.0]butyl radical  
294 cations can be built upon.

295

## 296 Methods

297 To an oven-dried 10 mL Schlenk tube equipped with a Teflon-coated magnetic stir bar was  
298 added  $[\text{Mes}_2\text{Acr}^t\text{Bu}_2]\text{ClO}_4$  (12.6 mg, 20.0  $\mu\text{mol}$ , 10 mol%), the respective olefin **2** (10.0 mmol, 10.0 equiv),  
299 and bicyclo[1.1.0]butane (BCB) **1a** (37.7 mg, 0.200 mmol, 1.00 equiv). The Schlenk tube was evacuated  
300 and backfilled with argon three times before  $\text{MeNO}_2$  (2.0 mL) was added under a positive argon pressure.  
301 The reaction mixture was stirred under irradiation with blue LEDs (18 W,  $\lambda_{\text{max}} = 425 \text{ nm}$ ) for 16 h. After this  
302 time, the solvent was removed under reduced pressure and the crude product was purified by flash  
303 column chromatography on silica gel to yield the corresponding bicyclo[2.1.1]hexane (**3**).

## 304 References

- 305 1. Wiberg, K. B. & Ciula, R. P. Ethyl bicyclo[1.1.0]butane-1-carboxylate. *J. Am. Chem. Soc.* **81**, 5261–  
306 5262 (1959).
- 307 2. Golfmann, M. & Walker, J. C. L. Bicyclobutanes as unusual building blocks for complexity generation  
308 in organic synthesis. *Commun. Chem.* **6**, 9 (2023).
- 309 3. Kelly, C. B., Milligan, J. A., Tilley, L. J. & Sodano, T. M. Bicyclobutanes: from curiosities to versatile  
310 reagents and covalent warheads. *Chem. Sci.* **13**, 11721–11737 (2022).
- 311 4. Fawcett, A. Recent advances in the chemistry of bicyclo- and 1-azabicyclo[1.1.0]butanes. *Pure Appl.*  
312 *Chem.* **92**, 751–765 (2020).
- 313 5. Tyler, J. L. & Aggarwal, V. K. Synthesis and applications of bicyclo[1.1.0]butyl and  
314 azabicyclo[1.1.0]butyl organometallics. *Chem. Eur. J.* **29**, e202300008 (2023).
- 315 6. Turkowska, J., Durka, J. & Gryko, D. Strain release - an old tool for new transformations. *Chem.*  
316 *Commun.* **56**, 5718–5734 (2020).

- 317 7. Lopchuk, J. M. *et al.* Strain-release heteroatom functionalization: development, scope, and  
318 stereospecificity. *J. Am. Chem. Soc.* **139**, 3209–3226 (2017).
- 319 8. Gianatassio, R. *et al.* Strain-release amination. *Science* **351**, 241–246 (2016).
- 320 9. Bellotti, P. & Glorius, F. Strain-release photocatalysis. *J. Am. Chem. Soc.* **145**, 20716–20732 (2023).
- 321 10. Ma, X., Sloman, D. L., Han, Y. & Bennett, D. J. A selective synthesis of 2,2-  
322 difluorobicyclo[1.1.1]pentane analogues: "BCP-F2". *Org. Lett.* **21**, 7199–7203 (2019).
- 323 11. Bychek, R. M. *et al.* Difluoro-substituted bicyclo[1.1.1]pentanes for medicinal chemistry: design,  
324 synthesis, and characterization. *J. Org. Chem.* **84**, 15106–15117 (2019).
- 325 12. McNamee, R. E., Thompson, A. L. & Anderson, E. A. Synthesis and applications of polysubstituted  
326 bicyclo[1.1.0]butanes. *J. Am. Chem. Soc.* **143**, 21246–21251 (2021).
- 327 13. Agasti, S. *et al.* A catalytic alkene insertion approach to bicyclo[2.1.1]hexane bioisosteres. *Nat.*  
328 *Chem.* **15**, 535–541 (2023).
- 329 14. Yan, H., Liu, Y., Feng, X. & Shi, L. Hantzsch esters enabled  $[2\pi+2\sigma]$  cycloadditions of bicyclo [1.1.0]  
330 butanes and alkenes under photo conditions. *Org. Lett.* **25**, 8116–8120 (2023).
- 331 15. Radhoff, N., Daniliuc, C. G. & Studer, A. Lewis acid catalyzed formal (3+2)-cycloaddition of  
332 bicyclo[1.1.0]butanes with ketenes. *Angew. Chem. Int. Ed.* **62**, e202304771 (2023).
- 333 16. Ni, D. *et al.* Intermolecular formal cycloaddition of indoles with bicyclo[1.1.0]butanes by Lewis acid  
334 catalysis. *Angew. Chem. Int. Ed.* **62**, e202308606 (2023).
- 335 17. Tang, L. *et al.* Silver-catalyzed dearomative  $[2\pi+2\sigma]$  cycloadditions of indoles with bicyclobutanes:  
336 access to indoline fused bicyclo[2.1.1]hexanes. *Angew. Chem. Int. Ed.* **62**, e202310066 (2023).
- 337 18. Liang, Y., Paulus, F., Daniliuc, C. G. & Glorius, F. Catalytic formal  $[2\pi+2\sigma]$  cycloaddition of aldehydes  
338 with bicyclobutanes: expedient access to polysubstituted 2-oxabicyclo[2.1.1]hexanes. *Angew.*  
339 *Chem. Int. Ed.* **62**, e202305043 (2023).
- 340 19. Liu, Y. *et al.* Pyridine-boryl radical-catalyzed  $[2\pi + 2\sigma]$  cycloaddition of bicyclo[1.1.0]butanes with  
341 alkenes. *ACS Catal.* **13**, 5096–5103 (2023).
- 342 20. Xu, M. *et al.* Diboron(4)-catalyzed remote [3+2] cycloaddition of cyclopropanes via  
343 dearomative/rearomative radical transmission through pyridine. *Angew. Chem. Int. Ed.* **61**,  
344 e202214507 (2022).
- 345 21. Guo, R. *et al.* Strain-release  $[2\pi + 2\sigma]$  cycloadditions for the synthesis of bicyclo[2.1.1]hexanes  
346 initiated by energy transfer. *J. Am. Chem. Soc.* **144**, 7988–7994 (2022).
- 347 22. Rossi, A. R., Wang, Y. & Wiberg, K. B. Excited states and photochemistry of bicyclo[1.1.0]butane. *J.*  
348 *Phys. Chem. A* **113**, 1686–1695 (2009).
- 349 23. Tokunaga, K. *et al.* Bicyclobutane carboxylic amide as a cysteine-directed strained electrophile for  
350 selective targeting of proteins. *J. Am. Chem. Soc.* **142**, 18522–18531 (2020).
- 351 24. Schwartz, B. D., Smyth, A. P., Nashar, P. E., Gardiner, M. G. & Malins, L. R. Investigating  
352 bicyclobutane-triazolinedione cycloadditions as a tool for peptide modification. *Org. Lett.* **24**, 1268–  
353 1273 (2022).

- 354 25. Dhake, K. *et al.* Beyond bioisosteres: divergent synthesis of azabicyclohexanes and cyclobutenyl  
355 amines from bicyclobutanes. *Angew. Chem. Int. Ed.* **61**, e202204719 (2022).
- 356 26. Gassman, P. G., Mullins, M. J., Richtsmeier, S. & Dixon, D. A. Effect of alkyl substitution on the ease  
357 of oxidation of bicyclo[1.1.0]butanes. Experimental verification of PRDDO calculations for the  
358 nature of the HOMO of bicyclo[1.1.0]butane. *J. Am. Chem. Soc.* **101**, 5793–5797 (1979).
- 359 27. Gassman, P. G. & Yamaguchi, R. Electrochemical oxidation of strained hydrocarbons. *J. Am. Chem.*  
360 *Soc.* **101**, 1308–1310 (1979).
- 361 28. Concurrent with the work presented in this manuscript, bicyclobutyl radical cations were suggested  
362 as a possible intermediate in the dearomatizing cycloaddition reaction of bicyclobutane and  
363 phenols. See Dutta, S. *et al.* Photoredox-enabled dearomative  $[2\pi + 2\sigma]$  cycloaddition of phenols. *J.*  
364 *Am. Chem. Soc.* **146**, 2789–2797 (2024). However, in this study it is stated that oxidation of the  
365 phenol fragment is equally feasible as a mechanistic pathway.
- 366 29. Gassman, P. G. & Carroll, G. T. The reaction of 1,2,2-trimethylbicyclo[1.1.0]butane with excited  
367 state 1-cyanonaphthalene. *Tetrahedron* **42**, 6201–6206 (1986).
- 368 30. Gassman, P. G., Olson, K. D., Walter, L. & Yamaguchi, R. Photoexcitation of nonconjugated,  
369 strained, saturated hydrocarbons. Relationship between ease of oxidation and the quenching of  
370 naphthalene fluorescence by saturated hydrocarbons. *J. Am. Chem. Soc.* **103**, 4977–4979 (1981).
- 371 31. Gassman, P. G. & Olson, K. D. Photochemistry of saturated hydrocarbons. Mechanistic changes as a  
372 function of methyl substitution in the photosensitized reactions of the tricyclo[4.1.0.02,7]heptyl  
373 system. *J. Am. Chem. Soc.* **104**, 3740–3742 (1982).
- 374 32. Saettel, N. J. & Wiest, O. Sterically crowded bicyclo[1.1.0]butane radical cations. *J. Org. Chem.* **68**,  
375 4549–4552 (2003).
- 376 33. Denisenko, A., Garbuz, P., Shishkina, S. V., Voloshchuk, N. M. & Mykhailiuk, P. K. Saturated  
377 bioisosteres of ortho-substituted benzenes. *Angew. Chem. Int. Ed.* **59**, 20515–20521 (2020).
- 378 34. Herter, L., Koutsopetras, I., Turelli, L., Fessard, T. & Salomé, C. Preparation of new  
379 bicyclo[2.1.1]hexane compact modules: an opening towards novel sp<sup>3</sup>-rich chemical space. *Org.*  
380 *Biomol. Chem.* **20**, 9108–9111 (2022).
- 381 35. Mykhailiuk, P. K. Saturated bioisosteres of benzene: where to go next? *Org. Biomol. Chem.* **17**,  
382 2839–2849 (2019).
- 383 36. Rigotti, T. & Bach, T. Bicyclo[2.1.1]hexanes by visible light-driven intramolecular crossed  $[2 + 2]$   
384 photocycloadditions. *Org. Lett.* **24**, 8821–8825 (2022).
- 385 37. Kleinmans, R. *et al.* Intermolecular  $[2\pi+2\sigma]$ -photocycloaddition enabled by triplet energy transfer.  
386 *Nature* **605**, 477–482 (2022).
- 387 38. Kleinmans, R. *et al.* ortho-Selective dearomative  $[2\pi + 2\sigma]$  photocycloadditions of bicyclic aza-  
388 arenes. *J. Am. Chem. Soc.* **145**, 12324–12332 (2023).
- 389 39. Dutta, S. *et al.* Double strain-release  $[2\pi+2\sigma]$ -photocycloaddition. *J. Am. Chem. Soc.* **146**, 5232–  
390 5241 (2024).

- 391 40. Robichon, M. de *et al.* Enantioselective, intermolecular  $[\pi 2 + \sigma 2]$  photocycloaddition reactions of  
392 2(1H)-quinolones and bicyclo[1.1.0]butanes. *J. Am. Chem. Soc.* **145**, 24466–24470 (2023).
- 393 41. Ischay, M. A., Ament, M. S. & Yoon, T. P. Crossed intermolecular [2+2] cycloaddition of styrenes by  
394 visible light photocatalysis. *Chem. Sci.* **3**, 2807–2811 (2012).
- 395 42. Ischay, M. A., Lu, Z. & Yoon, T. P. [2+2] cycloadditions by oxidative visible light photocatalysis. *J.*  
396 *Am. Chem. Soc.* **132**, 8572–8574 (2010).
- 397 43. Lin, S., Ischay, M. A., Fry, C. G. & Yoon, T. P. Radical cation Diels-Alder cycloadditions by visible light  
398 photocatalysis. *J. Am. Chem. Soc.* **133**, 19350–19353 (2011).
- 399 44. Kranz, D. P. *et al.* Molecular oxygen as a redox catalyst in intramolecular photocycloadditions of  
400 coumarins. *Angew. Chem. Int. Ed.* **51**, 6000–6004 (2012).
- 401 45. Poplata, S., Tröster, A., Zou, Y.-Q. & Bach, T. Recent advances in the synthesis of cyclobutanes by  
402 olefin [2 + 2] photocycloaddition reactions. *Chem. Rev.* **116**, 9748–9815 (2016).
- 403 46. Wang, X. & Chen, C. An approach for the synthesis of nakamuric acid. *Tetrahedron* **71**, 3690–3693  
404 (2015).
- 405 47. Pitzer, L., Sandfort, F., Strieth-Kalthoff, F. & Glorius, F. Carbonyl-olefin cross-metathesis through a  
406 visible-light-induced 1,3-diol formation and fragmentation sequence. *Angew. Chem. Int. Ed.* **57**,  
407 16219–16223 (2018).
- 408 48. Pitzer, L., Schäfers, F. & Glorius, F. Rapid assessment of the reaction-condition-based sensitivity of  
409 chemical transformations. *Angew. Chem. Int. Ed.* **58**, 8572–8576 (2019).

410

## 411 **Acknowledgements**

412 Generous financial support from the Alexander von Humboldt Foundation (J.L.T.) and the European  
413 Research Council (ERC Advanced Grant Agreement No. 101098156, HighEnT) are gratefully acknowledged.  
414 DFT calculations were performed on the IDRE Hoffman2 cluster at the University of California, Los Angeles,  
415 and the Extreme Science and Engineering Discovery Environment (XSEDE), which is supported by the  
416 National Science Foundation (OCI1053575). Additional funding was provided to K.N.H. by the NSF  
417 (CHE2153972). We sincerely thank Dr. Alessia Petti, Dr. Chetan C. Chintawar, Subhabrata Dutta, Johannes  
418 Erchinger and Christian Gutheil (Universität Münster) for helpful discussions.

## 419 **Author contributions**

420 J.L.T., F.S. and F.G. conceived the project. J.L.T. and F.S. designed the experiments and performed initial  
421 screening studies. J.L.T., F.S. and C.S. performed synthetic experiments. F.G. coordinated the project. K.H.,  
422 H.S. and A.W. conducted DFT calculations. C.G.D. analysed X-ray structures. J.L.T. wrote the manuscript,  
423 with contributions from all authors.

## 424 **Competing interests**

425 The authors declare no competing interests.

426 **Data availability**

427 CIF crystallographic data files and xyz coordinates of the optimised structures are available as  
428 Supplementary Files. Crystallographic data for the structures reported in this article have been deposited  
429 at the Cambridge Crystallographic Data Centre, under deposition numbers CCDC 2331780 (**5r**), 2331781  
430 (**5ad**), 2331782 (**5ad'**) and 2331783 (**5au**).

431